Macromolecules
ARTICLE

Macromolecules **2010**, *43*, 9865–9873 **9865**
DOI: 10.1021/ma101098d

Delayed Glassification Model for Free-Surface Suppression of T_g in Polymer Glasses

Scott T. Milner*,† and Jane E. G. Lipson*,‡

†*Department of Chemical Engineering, The Pennsylvania State University, University Park, Pennsylvania 16802, United States, and* ‡*Department of Chemistry, Dartmouth College, Hanover, New Hampshire 03755, United States*

Received May 18, 2010; Revised Manuscript Received September 15, 2010

ABSTRACT: Suppression of the glass transition by some tens of degrees within a few tens of nanometers of a free surface in a polymer film is a technologically important, commonly observed, as-yet poorly understood phenomenon. We construct a quantitative theory of the influence of the free surface via transmission of "kinks" or "free volume" along the backbone of loops starting and ending at the free surface, following a proposal by de Gennes. Using our delayed glassification (DG) model, we predict depth-dependent values of the local T_g for both semi-infinite and freestanding film geometries, for both infinite and finite molecular weights. The qualitative features of our results are in reasonable agreement with experiment, but the averaging process inherent in connecting our results to macroscopic observations raises further issues, which we treat in the following paper.

1. Introduction

Shifts of the glass transition in polymer thin films have been a subject of continuing interest and study.[1,2] A variety of experimental techniques have been employed to observe both globally averaged and more localalized measures of T_g in both freestanding[3−6] and supported[7−14] films.

One category of experiments measures the thickness of a thin film (freestanding or supported) as a function of temperature (the most common routes being by ellipsometry[3,4,6−8,10] or X-ray reflectivity[5,9]), and detects the glass transition as a reduction in the thermal expansion coefficient on cooling. A more localized probe of T_g has been achieved[11−14] by doping a layer within a supported film with fluorophores, and observing changes in the fluorophore spectrum caused by changes in local density.

The majority of evidence suggests that a strongly adsorbing substrate locally elevates T_g, while a free surface locally lowers T_g. The magnitude of the effect is typically tens of degrees kelvin, and the range of the effect typically tens of nanometers. However, no consistent explanation has emerged to account for interfacial effects. Another puzzling observation is that polymer molecular weight appears to play an important role in studies of the average T_g of freestanding films yet appears to play little or no role in the case of supported films.

The most reliable, uncontroversial experimental finding is that the free surface of a polymer film lowers the glass transition locally. In particular, more localalized probes of T_g near the surface of thick supported polymer films can be made on samples that have been well annealed. This avoids limitations on the annealing history imposed by dewetting from substrates, or hole formation in thin freestanding films. The results of such experiments are qualitatively consistent with other observations of T_g reduction near free surfaces.

The state of theory in explaining even this most prevalent result is unsatisfactory. In a previous paper,[15] we showed that the so-called "percolation model" of the effect of proximate interfaces on T_g could not explain the range and magnitude of reduction of T_g near a free surface. There are few published models for such effects;[16−18] the most frequently cited potential explanation of experimental observations is the "slip mechanism" of de Gennes.[16,17] However, this mechanism has never before been fully implemented as a model in a systematic calculation of local or average T_g, and compared to experiment—which is the goal and the accomplishment of this paper and the companion paper that follows.

*To whom correspondence should be addressed. E-mail: (S.T.M.) stm9@engr.psu.edu; (J.E.G.L.) Jane.Lipson@Dartmouth.edu.

2. Delayed Glassification Model

The "slip mechanism" of de Gennes'[16,17] is a proposal by which a free surface of a glassy polymer film leads to greater mobility in the nearby material. The physical idea is as follows. The immediate vicinity of the free surface of a polymer film on the scale of a few angstroms is posited to be fluidized, by virtue of the decreased density at the edge of the film (or the absence of immobilized glassy neighboring segments above). de Gennes postulated that a portion of a polymer chain forming a loop that begins and ends at the free surface can transport "kinks" (or "free volume", or some equivalent concept) along its own length, with a lower barrier for mobility than impedes segmental motion in a bulk sample. (This motion can be thought of as analogous to reptation, but with a tube diameter of monomeric dimensions.) The free surface is presumed to provide both a source and a sink of kinks. The result is a suppression of (i.e., delay in) the transition to the glass (glassification), hence our choice of the name delayed glassification (DG) model.

For a loop to be effective in plasticizing the material through which it passes, the characteristic relaxation time for a kink to diffuse the length of the loop must be less than the measurement time scale τ^*. The loop characteristic time is evidently an increasing function of loop length n and a decreasing function of temperature T. At any given temperature, there is a characteristic loop length $N^*(T)$ for which the relaxation time equals τ^*. Furthermore, there is a longest relevant loop N^*, given by $N^*(T_g^b)$, for which the loop relaxation time equals τ^* at the bulk

Published on Web 11/15/2010

glass transition temperature, T_g^b. Loops longer than this are never relevant in plasticizing near the free surface, because they become too slow to be effective for temperatures at or above T_g^b.

The magnitude of N^* controls the range of distances from a free surface at which the glass transition temperature will be reduced, within the DG model. The distance scale, we shall show below, is simply the root-mean-square radius of gyration of a random walk chain segment of length N^*. Evidently, for qualitative agreement with experiments that show a reduction of T_g over a distance of some tens of nanometers from a free surface, N^* must be taken to be quite large, corresponding to molecular weights in the range of 10^5-10^6g/mol.

If the typical molecular weight in the sample is smaller than N^*, then some of the loops that would have been active in a sample of infinite molecular weight will be broken by interruptions in the chain. Therefore, it is a robust feature of the DG model that the penetration depth of T_g reduction will be less in samples of lower molecular weight. Furthermore, since N^* is expected to be large, the range of molecular weight over which we expect a theory based on the DG model to give molecular weight dependence, will also be large.

de Gennes in his two papers provided some of the elements needed to construct a quantitative theory of T_g reduction for the proposed slip mechanism, but much remained to be specified and worked out. The necessary components of the DG theory are as follows:

- a model for $N^*(T)$, the length of the longest "fast loop" as a function of temperature;
- a calculation of the probability $P(z)$ for a chain segment at depth z in a sample to be on a fast loop;
- a criterion for the fraction of fast segments (segments on fast loops) in a local region sufficient to plasticize that region.

In this paper, we construct these necessary ingredients of our DG model, which is a complete theory incorporating the slip mechanism, and use them to calculate local $T_g(z)$ profiles for both semi-infinite and slab geometries, for both infinite and finite molecular weights. In section 3, we state a criterion based on the first-passage time for kinks diffusing along a loop from a (reflecting) source to an (absorbing) sink, to relate the loop relaxation time to a distribution of local segmental relaxation times. (Appendix A provides details of the first-passage time calculations.) We calculate the probability that a loop of length n is faster than τ^* at temperature T. We then discuss the temperature dependence of the local relaxation times, which ultimately determine the temperature dependence of $N^*(T)$.

In section 4, we use the random-walk statistics of chain segments in a melt and the method of images to determine $L(z,n)$, the probability that a chain segment at depth z from a free surface is on a loop of length n starting and ending at the free surface. (Details of the loop geometry calculations for both semi-infinite and finite slab geometries are presented in Appendix B.) Combining these results with our expression for the probability that a loop of length n is fast, we calculate the probability $P(z)$ that a segment at a depth z in the sample is on a fast loop. In section 5, we extend these results to the case of finite molecular weight, assuming a most-probable (exponential) chain length distribution.

In section 6, we present a simple criterion for plasticization of a region by the kink diffusion along loops, and present results for the local T_g as a function of depth z below the free surface of a semi-infinite polymer film. We compare results for infinite and finite molecular weights. In section 7, we present corresponding results for the local $T_g(z)$ in a finite slab of thickness h.

Finally, in section 8 we note several issues that arise from implementation of the DG model, including (1) the appropriate way to average the local $T_g(z)$ to obtain a global value suitable for comparison with macroscopic experiments, (2) whether the various T_g experiments are measuring the same thing, and (3) whether local relaxation times that enter the DG model should be functions only of the temperature (as the model assumes) or also the local environment itself.

3. Kink Diffusion

Consider the diffusive motion of a kink or some other localized degree of freedom along the contour length of a loop originating at and returning to the free surface. As it diffuses, the kink encounters different local regions along the chain, which may have different local relaxation times. We would like to characterize the relaxation time of the loop with respect to kink transmission by a single time scale, which will necessarily be some average over the different local time scales, and ought to scale in some way with the loop length.

In refs 16 and 17, de Gennes argued that the condition for a loop to be faster than the experimental time scale was simply that all of the segments along the loop needed to have local relaxation times that were shorter than the experimental time scale. That is, he assumed that loops would typically be made slow by the incoherent action of one or more very slow segments, rather than the collective slowing effect of many somewhat slow segments.

He asserted that the probability $F(n)$ that a loop of length n was fast was equal to p^n, where p is the probability that a segment along the loop is fast (relaxes more quickly than τ^*), which leads directly to an exponential dependence of $F(n) = \exp(-n/N^*)$ on loop length n (with the characteristic loop length N^* equal to $-\log p$). Here, we examine this assumption more closely, and ask whether it is consistent with a more specific model of the diffusion of kinks along a loop.

We propose that an appropriate time scale for kink transmission along a loop is the first-passage time for a kink "injected" at one end to diffuse to the other end. We model this with a diffusion problem in which the local kink diffusivity l_0^2/τ_i varies with monomer index i along the chain, with values for τ_i drawn from some distribution $p(\tau)$ of local relaxation times. In Appendix A, we show that the mean first-passage time is given in terms of the local relaxation times τ_i as

$$\tau = n^2\langle\tau_i\rangle = n\sum_i \tau_i \tag{1}$$

Since we are working with the assumption that the local relaxation times are random, the loop relaxation time is random as well, with a distribution $P(\tau)$ given formally as

$$P(\tau) = \int \mathrm{d}\tau_1 ... \mathrm{d}\tau_n \, \delta(n\sum_i \tau_i - \tau) p(\tau_1) ... p(\tau_n) \tag{2}$$

The criterion for a loop to be "fast" is that its relaxation time is less than the experimental time τ^*. Hence the probability $F(n;T)$ that a loop is fast is the partial integral of the relaxation time distribution:

$$F(n;T) = \int_0^{\tau^*} \mathrm{d}\tau' \, P(\tau';T) \tag{3}$$

in which the temperature dependence is ultimately contained only in the local relaxation time distribution $p(\tau;T)$.

To proceed further, we must specify some features of the local relaxation time distribution. The local relaxation time distribution is certainly at least as broad as an exponential, which would arise from uncorrelated waiting times for infrequent "hopping" events. But if the local dynamics are sufficiently heterogeneous, the resulting correlations between hopping events will lead to

a broader distribution, in which longer waiting times are more common than predicted by an exponential decay.

The form of the local relaxation time distribution $p(\tau)$ controls the distribution of loop relaxation times $P(\tau)$. For local relaxation time distributions with finite first and second moments (such that the central limit theorem applies), the form of $P(\tau)$ for large n approaches a Gaussian; this leads ultimately to $F(n;T)$ approaching a sharp cutoff (theta function) for large n.

Only for $P(\tau)$ sufficiently broad that no first moment exists does one obtain a form for $F(n;T)$ similar to the exponential decay posited by de Gennes in refs 16 and 17. For any plausible distribution for the local relaxation times—including exponential, stretched exponential, log-normal—the central limit theorem applies, and the form of $F(n;T)$ approaches a theta function $\Theta(N^*(T)-n)$.

The characteristic fast loop length $N^*(T)$ is a function of the local relaxation time distribution, and thereby the temperature. As the temperature decreases and the local relaxation times increase, $N^*(T)$ will evidently decrease. To determine $N^*(T)$ for a particular polymer system, we can either provide a model for the local relaxation times, or a scheme for extracting $N^*(T)$ from experimental data.

The simplest assumption is to take a WLF temperature dependence[19] for the local relaxation times, which we assume to be independent of z, so that in particular the mean local relaxation time goes as

$$\langle \tau_i \rangle = \tau_0 e^{A/(T-T_0)} \tag{4}$$

The temperature dependence of $N^*(T)$ would then follow [see eq 33] as

$$N^*(T) = \sqrt{\tau^*/\tau_0}\, e^{-A/(2(T-T_0))} \tag{5}$$

In keeping with de Gennes' hypothesis that kink transmission is less hindered than ordinary local relaxations in the bulk in polymers approaching the glass transition, we may expect that the WLF parameter A (and perhaps T_0 as well) would be smaller for slip motion than for typical glassy relaxation. Thus, this simple approach results in one or two adjustable parameters to capture the temperature dependence of the slip motion.

4. Loop Geometry

To compute the probability $P(z)$ that a segment at a height z is on a fast loop, we need to know the probability $L(z,n)$ that a segment at height z is on a loop of length n. Given that result, we can compute $P(z)$ by integrating over $L(z,n)$, times the probability $F(n;T)$ that a loop of length n is fast:

$$P(z) = \int_0^\infty dn\, L(z,n) F(n;T) \tag{6}$$

Assuming that $F(n;T)$ is well described by a theta function $\Theta(N^*(T) - n)$ as we have argued, we have

$$P(z) = \int_0^{N*(T)} dn\, L(z,n) \tag{7}$$

So we now turn our attention to computing $L(z,n)$, which has to do only with the geometry of random walks.

We compute $L(z,n)$ by considering the fate of a random walker launched from z, with an absorbing wall at the interface(s) of the sample. The probability that the walker reaches an interface between n and $n + dn$ steps is $A(z,n)$, the absorption rate. $A(z,n)$ is given in terms of the "survival probability" $S(z,n)$ that the walker has not yet reached the wall, by $A(z,n) = -\partial S(z,n)/\partial n$. Evidently, $A(z,n)$ is the probability distribution for the length of one-half of a loop containing a segment at height z. Thus, we may write

$$L(z,n) = \int_0^\infty dn_1 \int_0^\infty dn_2\, \delta(n_1 + n_2 - n) A(z,n_1) A(z,n_2) \tag{8}$$

We compute the absorption rate $A(z,n)$ by using the method of images. Details are given in Appendix B; the result is

$$A(z,n) = \sqrt{\frac{3}{2\pi}} \frac{z e^{-3z^2/2n}}{n^{3/2}} \tag{9}$$

We use this loop geometry result to compute $P(z)$ for the case of a semi-infinite slab, as follows. We take the Laplace transform of eq 8 with respect to n, to obtain $\tilde{L}(z,s) = \tilde{A}^2(z,s)$. The Laplace transform of $A(z,n)$ itself is

$$\tilde{A}(z,s) = \exp(-\sqrt{6s}z) \tag{10}$$

This we square, and invert the Laplace transform to obtain

$$L(z,n) = \sqrt{\frac{6}{\pi}} \frac{z e^{-6z^2/n}}{n^{3/2}} \tag{11}$$

Finally, we perform the integral in eq 7 to obtain the probability $P(z)$ that a segment a distance z from the interface is on a fast loop, as

$$P(z) = \mathrm{erfc}\left(\sqrt{\frac{6z^2}{N^*(T)}}\right) \tag{12}$$

We note that our result for $P(z)$ for a semi-infinite slab is a function of the ratio $z^2/N^*(T)$, a comparison of the distance from the interface z to the radius of gyration of the largest mobile loops.

For a finite slab, we once again calculate the absorption probability $A(z,n)$, this time using an eigenfunction expansion to solve the time-dependent diffusion equation. We again compute $L(z,n)$ by Laplace transform methods, and integrate eq 7 to obtain $P(z)$. The details are presented in Appendix B. The final result is

$$P(z) = \frac{16}{\pi^2} \sum_{\substack{k,k'=1 \\ k,k' \text{odd}}}^{\infty} \frac{kk'}{k^2 - k'^2} \sin\left(\frac{\pi k' z}{L}\right) \sin\left(\frac{\pi k z}{L}\right) \left(\frac{1 - e^{-k'^2 \pi^2 N^*/6L^2}}{k'^2} - \frac{1 - e^{-k^2 \pi^2 N^*/6L^2}}{k^2} \right) \tag{13}$$

5. Finite Molecular Weight

We extend the results of the previous section to finite molecular weight chains with an exponential chain length distribution, by writing the probability $P(z)$ as

$$P(z) = \int_0^{N*(T)} dn\, L(z,n) e^{-n/\overline{N}} \tag{14}$$

The final exponential factor expresses the probability that the loop on which the segment at height z sits in an infinite molecular-weight system, remains unbroken when we randomly cut chains to produce a sample of finite molecular weight. Here $\overline{N}$ is the mean chain length.

This leads directly to

$$P(z) = \sqrt{(6/\pi)} z \int_0^{N*(T)} dn\, n^{-3/2} e^{-6z^2/n} e^{-n/\overline{N}} \tag{15}$$

which cannot be expressed in closed form, but is amenable to numerical integration.

To obtain the corresponding result for a finite slab of thickness L, we again use eq 14, but with the expression for $L(z,n)$ from Appendix B appropriate to a finite slab. The result is

$$P(z) = \frac{16}{\pi^2}\sum_{\substack{k,k'=1\\ k,k' \text{odd}}}^{\infty} \frac{kk'}{k^2-k'^2}\sin\left(\frac{\pi k' z}{L}\right)\sin\left(\frac{\pi k z}{L}\right)$$

$$\times\left(\frac{1-e^{-k'^2\pi^2 N^*/6L^2}e^{-N^*/\overline{N}}}{k'^2+\overline{n}^{-1}} - \frac{1-e^{-k^2\pi^2 N^*/6L^2}e^{-N^*/\overline{N}}}{k^2+\overline{n}^{-1}}\right) \quad (16)$$

in which we have defined

$$\overline{n} = \frac{\pi^2\overline{N}}{6L^2} \quad (17)$$

6. Soft-Cutoff Approximation

Motivated by our analysis of the first-passage time for kink transmission, which supported a model in which the probability $F(N,T)$ of a loop of length N being fast was well approximated by a theta function, we have so far carried out our calculations with a "hard cutoff" for $F(N,T)$. This is computationally cumbersome; a more convenient approximation is to take a "soft" or exponential cutoff for $F(N,T)$, namely,

$$F(N,T) = \exp(-N/N^*(T)) \quad (18)$$

We now reprise the calculations of the previous two sections much more simply with the soft cutoff $F(N,T)$, and show by explicit comparison to the hard cutoff results that the soft cutoff approximation is sufficiently accurate for our purposes.

With eq 18 for $F(N,T)$, eqs 7 and 14 for $P(z)$ can be written in the same form,

$$P(z) = \int_0^\infty dn\, L(z,n)e^{-n/N_{\text{eff}}(T)} \quad (19)$$

in which we have defined

$$1/N_{\text{eff}}(T) = 1/N^*(T) + 1/\overline{N} \quad (20)$$

Thus, with the soft cutoff formulation, the effects on $P(z)$ of temperature and finite molecular weight are incorporated in a single parameter, a considerable simplification.

Using eq 8 for $L(z,n)$ in eq 19 above, we find the tidy result

$$P(z) = [\tilde{A}(z, 1/N_{\text{eff}}(T))]^2 \quad (21)$$

which holds both for semi-infinite films and for films of finite thickness. For the semi-infinite case, eq 10 leads immediately to

$$P(z) = \exp\left(-\sqrt{\frac{24z^2}{N_{\text{eff}}(T)}}\right) \quad (22)$$

For the finite-thickness case, we use eq 40 in eq 19 to obtain

$$P(z) = \left(\frac{4}{\pi}\sum_{\substack{k=1\\ k\text{odd}}}^{\infty}\frac{k\sin(k\pi z/L)}{k^2+n_{\text{eff}}^{-1}}\right)^2 \quad (23)$$

in which we have defined

$$n_{\text{eff}} = \frac{\pi^2 N_{\text{eff}}}{6L^2} \quad (24)$$

analogous to eq 17.

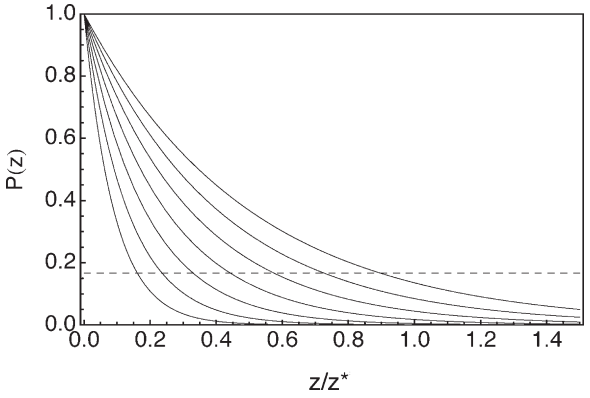

Figure 1. Probability $P(z)$ that a segment at depth z in a semi-infinite slab is on a fast loop, as a function of scaled depth z/z^*, for a set of representative temperatures, as described in main text. The dashed line represents plasticization criterion.

The sum in eq 23 can be evaluated in closed form (see Appendix C for details). The final result is

$$P(z) = \left(\cosh\left(\frac{\pi z}{\sqrt{n_{\text{eff}}}}\right) - \sinh\left(\frac{\pi z}{\sqrt{n_{\text{eff}}}}\right)\tanh\left(\frac{\pi}{2\sqrt{n_{\text{eff}}}}\right)\right)^2 \quad (25)$$

With this formula in hand, we can compare the soft-cutoff approximation results for $P(z)$ for finite thickness films, with the full hard-cutoff results. The correspondence between the soft- and hard-cutoff results is close enough to justify using the simpler approximation, which we adopt in the sections that follow.

The simplest geometry in which to explore effects of a free surface on local glass transition is a semi-infinite slab of material. We locate the local glass transition temperature $T_g(z)$ by finding the temperature at which the probability $P(z)$ of a segment at depth z being on a fast loop equals some threshold value p_c. The choice of p_c is somewhat arbitrary; we may argue that if more than a certain number of neighbors of a given monomer are on fast loops, then the entire local region should be regarded as plasticized. We choose $p_c = 1/6$, but our results are not particularly sensitive to this choice.

In Figure 1, we display results for $P(z)$ computed from eq 12 for the case of a semi-infinite slab and infinite molecular weight chains. The different curves correspond to successively lower temperatures, for which $N^*(T)$ is progressively smaller. We have measured the depth z from the free surface in units of z^*, defined to be the radius of gyration of a loop of length N^*, i.e., $z^{*2} = N^* b^2/6$. (Recall $N^* \equiv N^*(T_g^b)$ is the longest fast loop at the bulk glass transition.)

For this and other figures to follow, we have taken illustrative values for the parameters determining the temperature dependence of $N^*(T)/N^* = n^*(T)$, namely

$$n^*(T) = \exp(c(T-T_g)/(T-T_0))$$
$$c = 8$$
$$T_g = 373\ \text{K}$$
$$T_0 = T_g - 100\ \text{K} \quad (26)$$

The temperatures in Figure 1 are, from right to left, T_g, $T_g - 5$ K, and so forth down to $T_g - 30$ K. The dashed line shows the criterion $P(z) = p_c = 1/6$; the intersections of the curves with the dashed line determine the depth z that just becomes glassy at the given temperature. That is, we determine $T_g(z)$ by the requirement

$$P(z; T_g(z)) = p_c \quad (27)$$

Figure 2 shows the resulting family of curves for the local $T_g(z)$ relative to the bulk value T_g, as a function of reduced thickness

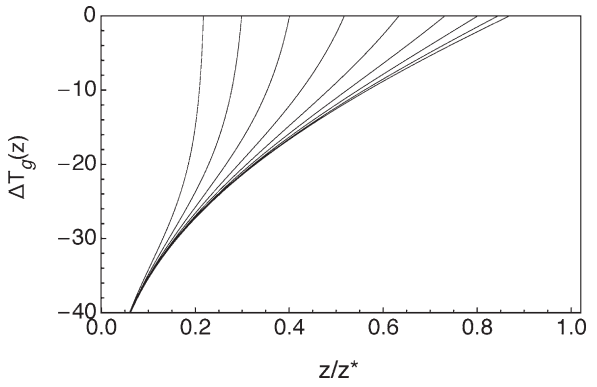

Figure 2. Local glass transition temperature shift $\Delta T_g(z)$ as a function of scaled depth z/z^*, for a representative set of mean molecular weights $\overline{N}/N^* = 1/16, 1/8, 1/4, 1/2, 1, 2, 4, 8, 16$.

z/z^*, for semi-infinite slabs of different molecular weight, computed from eqs 15 and 27. The number-averaged molecular weight $\overline{N}$ has been chosen to be a multiple of N^*; shown in the figure are curves for $\overline{N}/N^*$ equal to 1/16, 1/8, 1/4, 1/2, 1, 2, 4, 8, 16. The figure shows several characteristic behaviors of the curves that we expect based on the physics in the theory.

As an illustrative example, if we consider the sample to be comprised of polystyrene (PS) and take N^* to be 2.0×10^6 g/mol, then the range of average molecular weights represented in Figure 2 would span (left to right) from 1.25×10^5 to 3.2×10^7 g/mol, and the reduction parameter z^* would have a value of 38.0 nm.[20] Evidently, for larger molecular weights, the reduction of the local T_g extends deeper into the slab. However, this progression is eventually cut off, for chains much larger than N^*; long loops made on such chains can never be fast below the bulk T_g, and so are never effective in plasticizing material distant from the free surface.

For the smaller molecular weights, the curves are quite steep where the effect on T_g is cut off by the absence of longer loops (due to the absence of long enough chains). However, for those portions of the sample that are plasticized, the effect is as strong as for longer chains. This is because the loops that dominate in these regions are so short that they are insensitive to occasional breaks in the chain. On general grounds, we expect the curves to converge to the infinite-$\overline{N}$ result close to the free surface. Specifically, we expect this convergence to occur at distances where the typical loop length z is much smaller than the finite radius of gyration of the chain. Figure 2 displays this expected tendency for the local $T_g(z)$ curves to converge at small z.

7. Results for Finite Slab

Now we present results of our theory as applied to a finite slab, i.e., a free-standing film with its two free surfaces. We use the same criterion eq 27 for determining whether material at a depth z is plasticized.

Figure 3 displays representative curves for $P(z)$ in a finite slab, with chains of infinite molecular weight and a fixed value of N^*, for different layer thicknesses L. The layer thicknesses in the figure are multiples of the characteristic slab thickness L^*, defined equal to the radius of gyration of a chain segment of length N^*.

As we consider progressively thinner samples for the same value of N^* we see that the plasticizing effect of slip motion extends farther into the sample from both sides, until finally the entire sample may be affected.

The inset to Figure 3 shows the effect of finite molecular weight $\overline{N}$ on the shape of the $P(z)$ curve for a particular value of L, in this case $L = L^*$. The molecular weights shown are multiples of N^*; smaller values are the lower curves. Evidently, as $\overline{N}$ becomes comparable to or smaller than N^*, the plasticizing effect extends less into the sample.

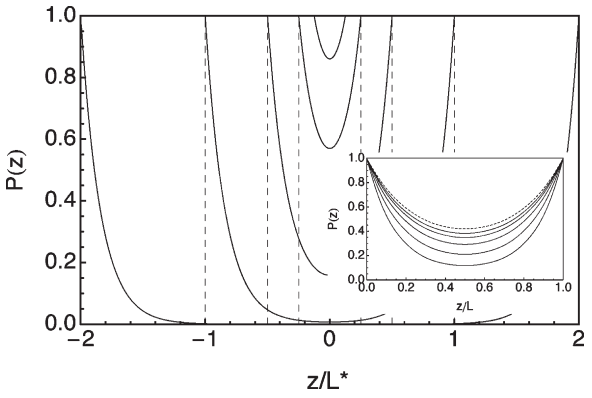

Figure 3. Representative curves of $P(z)$ in finite slabs of different thicknesses $L/L^* = {}^1/_4, {}^1/_2, 1, 2$, and 4, as a function of z/L^*. Inset: effect of finite $\overline{N}$ on the curve for $L = L^*$; here (from bottom to top) $\overline{N}/N^* = {}^1/_4, {}^1/_2, 1, 2, 4$, and ∞ (dashed).

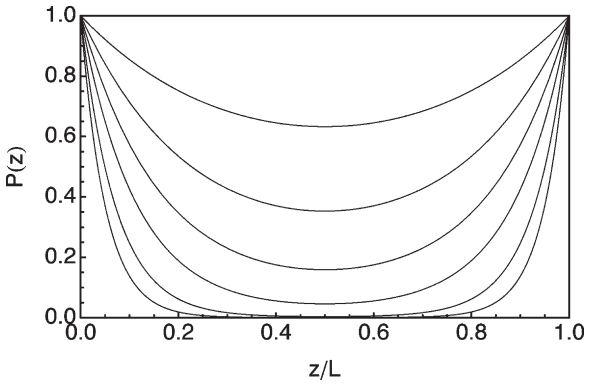

Figure 4. Representative curves of $P(z)$ in a finite slab of infinite molecular weight chains with different values of N^*, such that $N^*b^2/L^2 = 0.1, 0.2, 0.5, 1, 2, 5$.

Figure 4 presents another family of curves of $P(z)$, this time for a fixed slab thickness L (and infinite molecular weight), with different representative values of N^*, chosen as multiples of L^2/a^2 (i.e., the chain length such that the end-to-end distance is L).

As N^* increases, the plasticization effect extends increasingly into the sample.

On the basis of these results, we can apply our plasticization criterion to obtain characteristic curves for the local $T_g(z)$ within a finite slab. Figure 5 illustrates the typical behavior produced by our theory. Once again, we plot the shift in the local $T_g(z)$ relative to the bulk value T_g, for finite slabs of different thicknesses L, given in units of L^*. The abscissa is depth z in units of L^*; the thin dashed lines denote the boundaries of the various slabs considered.

In the inset to Figure 5, the effect of finite molecular weight is shown for a single representative slab thickness $L = 2L^*$. Molecular weights shown are $\overline{N}$ chosen as multiples of N^*, with $\overline{N}/N^* = 1/4, 1/2, 1, 2$, and 4.

Again, if we consider as an example a sample of PS such that $N^* = 2.0 \times 10^6$ g/mol then L^* would have a value of 38.0 nm.

In Figure 5, we can see that for sufficiently thick slab samples, the plasticization extends only into the near-surface region. In the center of a sufficiently thick sample (e.g., $L/L^* = 4$), the local glass transition occurs at the bulk T_g; we thus have a "sandwich" of plasticized and bulk-like material.

As we make the film thinner than L^*, loops and "bridges" (a chain segment spanning from one free surface to the other) are able to communicate across the entire sample. As a result, we find reduction of T_g across the entire sample thickness, with an increasingly uniform reduction as the sample becomes thinner.

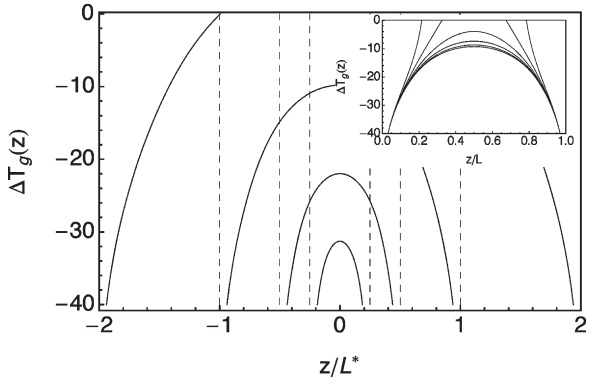

Figure 5. Local glass transition temperature $T_g(z)$ for finite slab samples of infinite molecular weight chains, with thicknesses $L/L^* = {}^1/_2$, 1, 2, and 4. Inset: effect of finite molecular weight on slab of thickness $L = 2L^*$, with (from top to bottom) $\overline{N}/N^* = 1/4, 1/2, 1, 2, 4$, and 8.

8. Discussion

In this paper, we have developed a theory based on the suggestion of de Gennes that a process of kink transmission, analogous to reptation in a polymer melt, may be responsible for plasticizing the near-surface region in a glassy polymer sample with a free surface. This "DG model" is our implementation of one of two oft-cited proposals in the literature for a microscopic, mechanistic explanation of how the free surface manages to lower the glass transition temperature some tens of nanometers deep into the film.

The other proposed explanation, based on the percolation model of Long and Lequeux,[21] we considered in an earlier paper.[15] There we showed that while the percolation model with reasonable parameter values could be consistent with the elevation of T_g in proximity to a strongly absorbing substrate, and it did predict a reduction of T_g at a free surface, neither the strength nor the range of the reduction was nearly enough to explain the experimental observations. So the kink transmission, which has been frequently cited by experimenters as a possible explanation of the free surface effect but never fully developed, is the only microscopic mechanism currently proposed that may be viable. Furthermore, kink transmission is the only approach yet proposed that contains a mechanism for molecular weight dependence of the T_g reduction extending to quite large molecular weights, which is a key feature of the ellipsometry studies of T_g in freestanding films. Thus, the slip mechanism both merits and requires a thorough theoretical treatment.

This paper provides that thorough treatment, via the development of the delayed glassification (DG) model. The parameters in the model are relatively few. We have N^*, the largest fast loop at the bulk T_g, which determines the maximum range of the free surface effect. Then, we have the temperature dependence of $N^*(T)$, which we have assumed to be of WLF form, eq 26. This introduces two more parameters—the WLF-like temperature T_0 at which $N^*(T)$ would in principle be driven to zero, and the energy parameter c. Because the slip mechanism is hypothesized to be active at temperatures at which a bulk sample would be glassy, we expect that c and possibly T_0 for the slip motion will be less than their counterparts for the usual WLF temperature dependence of the bulk glass transition.

Our DG model predicts the local $T_g(z)$, based on the criterion that a sufficient fraction of material at depth z within the sample is situated on a fast loop (or bridge, in the case of finite slab samples) and therefore plasticized by the transmission of kinks back and forth on the loop.

Our theory, indeed any quantitative theory based on the slip transmission idea, must have certain qualitative features. The range of reduction of T_g near a free surface will be determined by the value of N^*, specifically by the end-to-end distance of chain segment of this length. Because the experimental range of the lowering of T_g is of order tens of nanometers, N^* must be quite large, of order 10^5−10^6 g/mol.

If chains in a sample are shorter than this, then the range of free surface effects will be limited by $\overline{N}$. That is, no effect will persist far beyond the radius of gyration of the chains in the sample. Since N^* is large, the range of molecular weights over which a dependence on $\overline{N}$ of the local T_g will be relevant will likewise be large.

Moreover, our model results indicate that in freestanding films that are thin compared to the radius of gyration of typical chains in the sample, the molecular weight dependence ceases to have an impact. This is because all relevant loops and bridges in such a sample are far shorter than typical chains, and so unlikely to be interrupted by the end of a chain.

Our DG model-based observations have focused on our predictions for the local glass transition, $T_g(z)$. Of course, experiments do not measure the local T_g. Some experiments, such as ellipsometry or other determinations of film thickness, or dynamic heat capacity, measure some average of the glass transition through the sample.

The technique of fluorophore doping can in principle be used to determine a more localized T_g, or at least an average of $T_g(z)$ over a limited depth range. So far, it has most commonly been used in a mode in which a "reporting layer" (doped with fluorophore) of varying thickness comprises a portion of a much thicker supported sample. In these experiments as in the other experimental routes to T_g, there is an averaging process to be considered—and modeled theoretically—before a quantitative comparison to data can be made. This turns out to be a somewhat subtle problem, which is addressed in the companion paper that follows.

Finally, we note that an important implicit assumption of our DG model is that the local relaxation time distribution $p(\tau)$ is only a function of temperature, unaffected by the local environment. This precludes any effect of the local neighborhood of a segment on speeding up or slowing down its relaxation. Such collective effects are another possible route to explaining how the proximity of a free surface could lower the local glass transition. However, it is not clear whether there would be any role for molecular weight dependence in such a picture. We shall address this approach in future work.

Appendix A. First Passage Time

A fast loop is one in which a kink can manage to diffuse along the loop within the experimental time. The diffusion constant for the kink varies along the loop, because the barriers vary. We can define an average diffusion time for a kink along the loop in terms of the mean first passage time from one end of the loop to the other, as follows.

Imagine repeatedly injecting a kink (a random walker) at one end of a line, with a reflecting boundary condition where the kink is injected and an absorbing condition at the other end. Each kink will diffuse around for a while, and eventually be absorbed at the other end. There will be a probability distribution of absorption times; we seek the average time.

A simple way to compute this time is to solve a steady-state problem, in which we inject kinks at a rate J, which must be absorbed at the other end in steady state at the same rate J; we then compute the total number of kinks K all along the line. On average, if a kink survives a time τ before being absorbed, then if we inject kinks at a rate J, there must be $K = J\tau$ kinks present on the line in steady state. Hence the mean first passage time is then given by

$$1/\tau = J/K \tag{28}$$

We compute K, and then τ, as follows. In steady state, the current $J = -D(s)\partial\psi/\partial s$ is independent of arclength s (walkers do

not pile up anywhere). We can thus integrate for the concentration $\psi(s)$ as

$$\psi(s) = \int_s^L \frac{J}{D(s')}\,\mathrm{d}s' \tag{29}$$

K is then simply equal to the integral of $\psi(s)$ over the entire loop arclength L. (We have taken $s = L$ as the absorbing boundary, and $s = 0$ as the (reflecting) injection boundary.)

Using eqs 28 and 29, and the above result for K, we have after a bit of arithmetic

$$\tau = \int_0^L \frac{s}{D(s)}\,\mathrm{d}s \tag{30}$$

Since $D(s)$ is a random variable, i.e., the hopping rate and therefore the local diffusivity of kinks varies as a function of position along the loop, and we expect $D(s)$ values to be uncorrelated with s and with each other, we may write

$$\tau = \frac{L^2}{2}\left\langle \frac{1}{D} \right\rangle \tag{31}$$

Now the local diffusion constant $D(s)$ (or equivalently D_i, the diffusion constant near the ith monomer) may be written as $D_i = a^2/(2\tau_i)$, where τ_i is the hopping time at the ith monomer. Hence we have, finally,

$$\tau = N^2\langle \tau_i \rangle \tag{32}$$

The N^2 dependence in this result arises from diffusion along a path of length N monomers, and the characteristic time is proportional to the average local hopping time.

If we set the loop relaxation time τ equal to some experimental time scale τ^*, this determines a longest mobile loop length $N^*(T)$,

$$N^*(T) = \sqrt{\tau^*/\langle \tau_i \rangle} \tag{33}$$

which depends on temperature through the temperature dependence of the local relaxation times.

Appendix B. Loop Geometry

To compute the survival probability $S(z,n)$, we need the probability $P(z,z',n)$ that a walker launched at z reaches z' after n steps without reaching a wall. The survival probability $S(z,n)$ is the integral of $P(z,z',n)$ over all places z' the walker could be after n steps:

$$S(z,n) = \int \mathrm{d}z'\, P(z,z',n) \tag{34}$$

The function $P(z',z,n)$ is the solution to the diffusion equation with a delta-function initial condition $P(z',z,0) = \delta(z-z')$. For a semi-infinite slab with interface at $z = 0$, the solution is given in terms of the method of images, as

$$P(z',z,n) = \left(\frac{3}{2\pi n a^2}\right)^{1/2}\left[\exp\left(\frac{-3(z'-z)^2}{2na^2}\right) - \exp\left(\frac{-3(z'+z)^2}{2na^2}\right)\right] \tag{35}$$

The survival probability is (setting $a = 1$, i.e., measuring z in units of a)

$$S(z,n) = \mathrm{erf}\left(\sqrt{\frac{3z^2}{2n}}\right) \tag{36}$$

and the corresponding absorption probability $A(z,n) = -\partial S/\partial n$ is

$$A(z,n) = \sqrt{\frac{3}{2\pi}}\,\frac{z\mathrm{e}^{-3z^2/2n}}{n^{3/2}} \tag{37}$$

Now we treat the problem of random walkers in a slab of finite thickness L. We compute the probability $P(z',z,n)$ that a random walker launched at z' reaches z after n steps without being absorbed at either wall. From this, we can compute the survival probability $S(z,n)$ by integrating as before.

The probability distribution P satisfies the diffusion equation,

$$\frac{\partial P}{\partial n} = D\frac{\partial^2 P}{\partial z^2} \tag{38}$$

The diffusion constant D is chosen so that the solution to eq 38 in the absence of walls corresponds to a random walker with step length a. The free solution can be shown to be

$$P(z,n) \propto n^{-1/2}\mathrm{e}^{-z^2/(4Dn)} \tag{39}$$

which leads to the mean-square displacement in z being given by $\langle z^2 \rangle = 2Dn$. Whereas, we require that $\langle z^2 \rangle = (1/3)\langle r^2 \rangle$ and $\langle r^2 \rangle = na^2$ for an isotropic random walk of n steps and step length a. Hence $D = a^2/6$.

So we seek the solution of eq 38 with absorbing boundary conditions $P(z,n) = 0$ at $z = 0$ and $z = L$, and initial condition $P(z,0) = \delta(z-z')$. The boundary conditions suggest an expansion in sines,

$$P(z,n) = \sum_{k=1}^{\infty} p_k(n)\sin\left(\frac{k\pi z}{L}\right) \tag{40}$$

The completeness relation for sines expresses the delta function as

$$\delta(z-z_0) = \frac{2}{L}\sum_{k=1}^{\infty}\sin\left(\frac{k\pi z_0}{L}\right)\sin\left(\frac{k\pi z}{L}\right) \tag{41}$$

This allows us to set initial conditions for the Fourier coefficients $\{p_k(n)\}$ as

$$p_k(0) = \frac{2}{L}\sin\left(\frac{k\pi z_0}{L}\right) \tag{42}$$

Subsituting the sine series into the diffusion equation and equating like coefficients leads to a set of ordinary differential equations for the Fourier coefficients,

$$\frac{\partial p_k(n)}{\partial n} = -\frac{Dk^2\pi^2}{L^2}p_k(n) \tag{43}$$

which may be solved immediately. Substituting the solutions into the sine series for P gives the result

$$P(z_0,z,n) = \sum_{k=1}^{\infty}\frac{2}{L}\sin\left(\frac{\pi k z_0}{L}\right)\sin\left(\frac{\pi k z}{L}\right)\mathrm{e}^{-Dk^2\pi^2 n/L^2} \tag{44}$$

The survival probability is then given as

$$S(z,n) = \int_0^L \mathrm{d}z'\, P(z,z',n) \tag{45}$$

which leads to

$$S(z,n) = \sum_{\substack{k=1\\ k\text{odd}}}^{\infty} \frac{4}{\pi k} \sin\left(\frac{\pi k z}{L}\right) \exp\left(-\frac{Dk^2\pi^2 n}{L^2}\right) \tag{46}$$

The corresponding result for $A(z,n)$ is

$$A(z,n) = \sum_{\substack{k=1\\ k\text{odd}}}^{\infty} \frac{4D\pi k}{L^2} \sin\left(\frac{\pi k z}{L}\right) \exp\left(-\frac{Dk^2\pi^2 n}{L^2}\right) \tag{47}$$

The Laplace transform of $A(z,n)$ with respect to n gives

$$\tilde{A}(z,s) = \sum_{\substack{k=1\\ k\text{odd}}}^{\infty} \frac{4D\pi k}{L^2} \sin\left(\frac{\pi k z}{L}\right) \left(s + \frac{Dk^2\pi^2}{L^2}\right)^{-1} \tag{48}$$

This we square to obtain $\overline{L}(z,s)$; we invert the Laplace transform to find $L(z,n)$ as a double sum,

$$L(z,n) = \frac{16D}{L^2} \sum_{\substack{k,k'=1\\ k,k'\text{odd}}}^{\infty} \frac{kk'}{k^2-k'^2} \sin\left(\frac{\pi k' z}{L}\right) \sin\left(\frac{\pi k z}{L}\right) \left(e^{-Dk'^2\pi^2 n/L^2} - e^{-Dk^2\pi^2 n/L^2}\right) \tag{49}$$

This we may integrate to get $P(z)$, to obtain eq 13 in the main text.

Appendix C. Summation Details

Direct numerical evaluation of eq 13 poses difficulties. First of all, the term $k = k'$ must be evaluated by taking the limit $k \to k'$, since the term as written is indeterminate. More troublesome is the slow convergence of the sum as written. Truncating the sum at some $k,k' < k_{max}$ leads to spurious oscillations in the result. Also, we find Gibbs phenomenon for z approaching the boundaries, because $P(z)$ approaches unity there, but we have used a sine series for which every term vanishes on the boundary.

To deal with the Gibbs phenomenon, we can deal separately with the terms proportional to $1/k^2$ and $1/k'^2$. Using the identity $1/k^2 - 1/k'^2 = (k'^2-k^2)/(k^2k'^2)$, we see that this portion of the double sum factors into the square of a one-dimensional sum, which may be summed exactly:

$$P_1(z) = \frac{16}{\pi^2} \sum_{\substack{k,k'=1\\ k,k'\text{odd}}}^{\infty} \frac{kk'}{k^2-k'^2} \sin\left(\frac{\pi k' z}{L}\right) \sin\left(\frac{\pi k z}{L}\right) \left(\frac{1}{k'^2} - \frac{1}{k^2}\right)$$

$$= \left(\frac{4}{\pi} \sum_{\substack{k=1\\ k\text{odd}}}^{\infty} \frac{1}{k} \sin\left(\frac{\pi k z}{L}\right)\right)^2 = 1 \tag{50}$$

This eliminates the Gibbs phenomenon.

If we now sum the remaining terms numerically with a truncated sum, we still find slow convergence. The leading error by direct observation is proportional to $\cos((k_{max}+1)\pi z/L)$, which arises from the first neglected terms $k = k_{max} + 2, k' = 1$ and vice versa. The convergence is slow because this term has a coefficient of order $1/k$, which becomes small only slowly as k_{max} increases.

To remedy this, we extract some additional terms that may be summed exactly, making using of the identities

$$\frac{1}{k^2-k'^2} = \frac{1}{k^2} + \frac{\kappa'^2}{k^2(k^2-k'^2)}$$

$$\frac{1}{k^2-k'^2} = -\frac{1}{k'^2} + \frac{\kappa'^2}{k'^2(k^2-k'^2)} \tag{51}$$

Using these in the second and fourth terms respectively of eq 13, we find after some rearrangement

$$P(z) = 1 - \frac{8}{\pi} \sum_{\substack{k=1\\ k\text{odd}}}^{\infty} \frac{1}{k} \sin(\pi k z) e^{-k^2 n^*}$$

$$- \frac{16}{\pi^2} \sum_{\substack{k,k'=1\\ k,k'\text{odd}}}^{\infty} \frac{kk'}{k^2-k'^2} \sin(\pi k z) \sin(\pi k' z) \left(\frac{e^{-k'^2 n^*}}{k^2} - \frac{e^{-k^2 n^*}}{k'^2}\right) \tag{52}$$

in which we have taken z in units of L, and defined n^* as

$$n^* = \frac{\pi^2 N^*}{6L^2} \tag{53}$$

analogous to eq 17. The point of the rearrangement is that now the leading correction term in the double sum, i.e., the first term omitted when the sum is truncated, is of order $1/k_{max}^3$ rather than $1/k_{max}$, so that the convergence is much more rapid.

Similar considerations apply to the evaluation of eq 16, for $P(z)$ in the case of finite molecular weight chains. Again we deal with the Gibbs phenomenon by separately summing the first and third terms of the final factor, using the identity

$$\frac{1}{k'^2 + \overline{n}^{-1}} - \frac{1}{k^2 + \overline{n}^{-1}} = \frac{k^2 - k'^2}{(k'^2 + \overline{n}^{-1})(k^2 + \overline{n}^{-1})} \tag{54}$$

This again permits us to write this portion of the double sum as the square of a one-dimensional sum,

$$P_1(z) = \left(\frac{4}{\pi} \sum_{\substack{k=1\\ k\text{odd}}}^{\infty} \frac{k \sin(\pi k z)}{k^2 + \overline{n}^{-1}}\right)^2 \tag{55}$$

The sum within parentheses can be performed exactly, using the result[22]

$$S(x,\alpha) = \sum_{k=1}^{\infty} \frac{k \sin(kx)}{k^2+\alpha^2} = \frac{\pi \sinh \alpha(\pi - x)}{2 \sinh \alpha\pi} \tag{56}$$

We have evidently

$$\frac{4}{\pi} \sum_{\substack{k=1\\ k\text{odd}}}^{\infty} \frac{k \sin(\pi k z)}{k^2 + \overline{n}^{-1}} = \frac{4}{\pi}\left(S(\pi z, 1/\sqrt{\overline{n}}) - \frac{1}{2} S(2\pi z, 1/2\sqrt{\overline{n}})\right) \tag{57}$$

which leads to

$$\frac{4}{\pi} \sum_{\substack{k=1\\ k\text{odd}}}^{\infty} \frac{k \sin(\pi k z)}{k^2 + \overline{n}^{-1}} = \cosh\left(\frac{\pi z}{\sqrt{\overline{n}}}\right) - \sinh\left(\frac{\pi z}{\sqrt{\overline{n}}}\right) \tanh\left(\frac{\pi}{2\sqrt{\overline{n}}}\right) \tag{58}$$

(This result likewise gives eq 25 for the soft-cutoff case treated in section 6.)

The convergence of the remaining terms of $P(z)$ (second and fourth terms in eq 16) can be improved using eq 51 and a rearrangement similar to that which led to eq 52. The final result is

$$P(z) = \left(\cosh\left(\frac{\pi z}{\sqrt{\bar{n}}}\right) - \sinh\left(\frac{\pi z}{\sqrt{\bar{n}}}\right)\tanh\left(\frac{\pi}{2\sqrt{\bar{n}}}\right)\right)^2 - \frac{8}{\pi}e^{-n^*/\bar{n}}\sum_{\substack{k=1\\ k\text{odd}}}^{\infty}\frac{k\sin(\pi kz)}{k^2+\bar{n}^{-1}}e^{-k^2n^*}$$

$$-\frac{16}{\pi^2}e^{-n^*/\bar{n}}\sum_{\substack{k,k'=1\\ k,k'\text{odd}}}^{\infty}\frac{kk'}{k^2-k'^2}\sin(\pi kz)\sin(\pi k'z)\left(\frac{k'^2e^{-k'^2n^*}}{k^2(k'^2+\bar{n}^{-1})} - \frac{k^2e^{-k^2n^*}}{k'^2(k^2+\bar{n}^{-1})}\right) \quad (59)$$

As before, we see that the final sum now has a leading correction term of order $1/k_{max}{}^3$.

References and Notes

(1) Forrest, J.; Dalnoki-Veress, K. *Adv. Colloid Interface Sci.* **2001**, *94*, 167–196.
(2) Roth, C.; Dutcher, J. *J. Electroanal. Chem.* **2005**, *584*, 13–22.
(3) Dalnoki-Veress, K.; Forrest, J. A.; de Gennes, P. G.; Dutcher, J. R. *J. Phys. IV Fr.* **2000**, *10*, 221–226.
(4) Dalnoki-Veress, K.; Forrest, J. A.; Murray, C.; Gigault, C.; Dutcher, J. R. *Phys. Rev. E* **2001**, *63*, 031801.
(5) Miyazaki, T.; Inoue, R.; Nishida, K.; Kanaya, T. *Eur. Phys. J.* **2007**, *141*, 203.
(6) Roth, C. B.; Dutcher, J. *Eur. Phys. J.* **2003**, *12*, S103–S107.
(7) Keddie, J.; Jones, R.; Cory, R. *Europhys. Lett.* **1994**, *27*, 59.
(8) Tsui, O.; Zhang, H. *Macromolecules* **2001**, *34*, 9139–9142.
(9) Tsui, O.; Russell, T. P.; Hawker, C. J. *Macromolecules* **2001**, *34*, 5535.
(10) Sharp, J.; Forrest, J. *Phys. Rev. Lett.* **2003**, *91*, 235701.
(11) Ellison, C.; Torkelson, J. *Nat. Mat.* **2003**, *2*, 695.
(12) Ellison, C.; Mundra, M.; Torkelson, J. *Macromolecules* **2005**, *38*, 1767–1778.
(13) Mundra, M.; Ellison, C.; Rittigstein, P.; Torkelson, J. *Eur. Phys. J. Spec. Top.* **2007**, *141*, 143.
(14) Priestley, R.; Mundra, M.; Barnett, N.; Broadbelt, L.; Torkelson, J. *Aust. J. Chem.* **2007**, *60*, 765.
(15) Lipson, J. E. G.; Milner, S. T. *Eur. Phys. J. B* **2009**, *72*, 133–137.
(16) de Gennes, P. G. *C. R. Acad. Sci. Paris, Ser. IV* **2000**, *1*, 1179.
(17) de Gennes, P. G. *Eur. Phys. J. E* **2000**, *2*, 201.
(18) Stevenson, J. D.; Wolynes, P. G. *J. Chem. Phys.* **2008**, *129*, 234514.
(19) Ferry, J. D. *Viscoelastic properties of polymers*; Wiley: New York, 1980.
(20) Fetters, L.; Lohse, D.; Richter, D.; Witten, T.; Zirkel, A. *Macromolecules* **1994**, *27*, 4639–4647.
(21) Long, D.; Lequeux, F. *Eur. Phys. J. E.* **2001**, *4*, 371–387.
(22) Gradshteyn, I. S.; Ryzhik, I. M. *Table of Integrals, Series, and Products*; Academic Press: Orlando, FL, 1980; p 40.